

STERNBERG ASTRONOMICAL INSTITUTE  
MOSCOW STATE UNIVERSITY  
INSTITUTE OF ASTRONOMY  
RUSSIAN ACADEMY OF SCIENCES

# ASTRONOMY AT THE EPOCH OF MULTIMESSENGER STUDIES

Proceedings of the VAK-2021 conference,  
Aug 23–28, 2021

Edited by A.M. Cherepashchuk et al.

Moscow  
Janus-K  
2022

UDK 52  
BBK 22.6

**Astronomy at the epoch of multimessenger studies. Proceedings of the VAK-2021 conference,  
Aug 23–28, 2021** — Moscow, Janus-K, 2022 (486 pp.)

ISBN 978-5-8037-0848-3

**Edited by**

Cherepashchuk A.M., Emelyanov N.V., Fedorova A.A., Gayazov I.S., Ipatov A.V., Ivanchik A.V., Malkov O.Yu.,  
Obridko V.N., Rastorguev A.S., Samus N.N., Shematovich V.I., Shustov B.M., Silchenko O.K., Zasov A.V.

This volume contains papers based on talks presented at the Russian Astronomical Conference VAK-2021 and comprises a wide range of astronomical and astrophysical subjects.

© SAI MSU, INASAN, 2022

© Authors, 2022

# X-ray morphology of pulsar wind nebulae: the effect of local medium motion

K. Levenfish<sup>1</sup>, G. Ponomaryov<sup>1,2</sup>, A. Petrov<sup>1</sup>  
ksen@astro.ioffe.ru

<sup>1</sup>*Ioffe Institute, St. Petersburg, Russia*

<sup>2</sup>*Peter the Great St. Petersburg Polytechnic University, St. Petersburg, Russia*

The effect of the relative motion of the pulsar wind nebula (PWN) and the local medium on the PWN X-ray morphology is studied using relativistic MHD modelling. It is shown that even the slow (subsonic) motion may strongly affect the X-ray appearance of PWNe and the integral flux of their emission. Accounting for the relative motion is also necessary to avoid misinterpretation of the PWN structure.

*Keywords: pulsar wind nebulae, relativistic MHD simulations, PLUTO*

DOI: 10.51194/VAK2021.2022.1.1.109

## 1. Introduction

Pulsar wind nebulae (PWNe) are natural laboratories for studying relativistic magnetized plasma. In particular, by comparing the results of relativistic magnetohydrodynamic (RMHD) modeling with the PWNe observables – spectrum, dynamics, morphology. The correct interpretation of X-ray morphologies is crucial for understanding plasma processes and patterns in PWNe.

X-ray morphologies naturally fall into two groups depending on the Mach number of the PWNe motion relative to their surroundings [1]. At  $M \lesssim 1$ , nebulae tend to acquire a *jet-torus* structure with an X-ray morphology determined by the pulsar parameters – spin-down luminosity, initial pulsar wind magnetization  $\sigma_0$ , magnetic axis tilt  $\alpha$ , etc. At  $M \gg 1$ , nebulae drive a bow-shock ahead and acquire a cometary *head-tail* structure, in which jets and tori are usually crushed by the ram pressure of an ambient matter stream.

Slow PWNe with  $M \lesssim 1$  are usually modeled under assumption of stationary or radially expanding surroundings. But in fact, moving PWNe in their rest frame usually see the oncoming free stream of surrounding matter. We argue that the influence of such a stream must be taken into account in order to correctly determine the type of PWN (single- or double-torus) and to achieve better correspondence of the simulated and actual X-ray morphology of PWNe.

## 2. Results

### 2.1. Subsonic motion and PWN morphology

The effect of the free stream on the X-ray morphology is illustrated in figure 1, in panels (1) and (3). Shown are X-ray maps of the same PWN model, of the same age, viewed at the same aspect, and interacting with the same stream; only the directions of this stream are opposite, as shown by arrows. This stream is initiated in the entire computation domain before the PWN begins to evolve. (The RMHD model is built with the PLUTO code [2], with the setup as in [3]).

Clearly, the X-ray appearance of the PWN in panels (1) and (3) is drastically different; see [3] for detail. Depending on whether the PWN is facing us upwind or leeward, it can exhibit either a Crab-like or Vela-like morphology (these PWNe are shown in panels (2) and (4)). In the former case, the prominent X-ray features are: steady torus and inner ring of nearly uniform brightness, transient wisps, and bright SE jet with “sprite” at its base. In the latter case, PWN exhibits two steady bright arcs, bright NW jet and feeble SE counter-jet. Interestingly, that in both cases, only stream-facing (windward) jets appear bright, while counter-jets are faint and embedded in a diffuse structure.

Thus, taking into account the ram pressure of the ambient matter stream is important for avoiding misinterpretation (as single- or a double-torus objects) of those PWNe that are not resolved that well as the Crab and Vela nebulae.

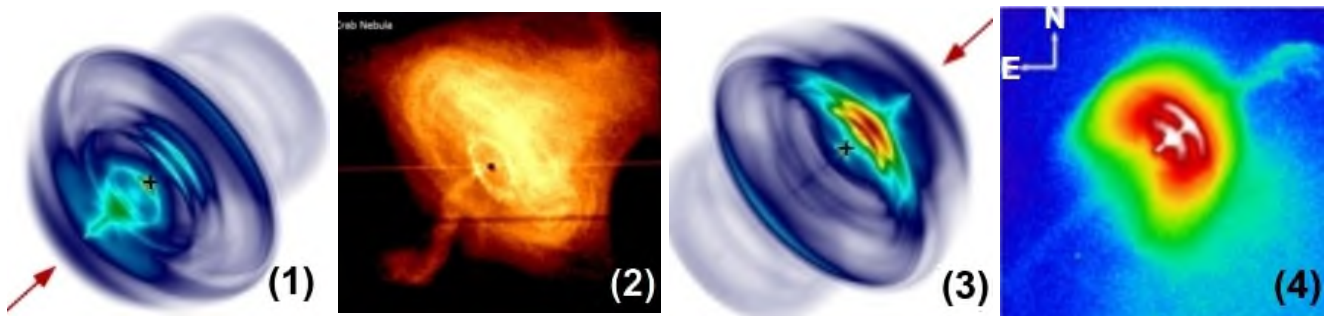


Figure 1: *Panels (1), (3)*: synthetic maps of synchrotron X-ray radiation of the same PWN model ( $\alpha = 45^\circ$ ,  $\sigma_0 = 0.03$ ) of age  $t = 14$  yr, which meets a subsonic flow of the surrounding matter having the same Mach number ( $M = 0.7$ ) but opposite direction (shown by red arrows). The PWN model is viewed at the same aspect as the Crab [4] and Vela PWNe, whose X-ray images are shown in *panels (2) and (4)*, respectively ( $\theta_{view} = 120^\circ$ ; the position angle is  $310^\circ$ , north through east).

## 2.2. The effect of the motion on the integral flux

The visible difference between the synthetic maps of the Crab-like and Vela-like models shown in Figure 1 translates into the difference of their integral X-ray fluxes by about (10-15)% (Figure 2). The flux is higher when the nebula is viewed from the leeward side (the Vela-like case). Both model PWNe exhibit variations of the integral fluxes of  $\sim 5\%$  on a year time-scale, due to reverberations of the torus. Thus, taking the motion into account can also be important for studying the variability of high-energy emission from PWNe. In particular, the observed variability of the Crab nebula, which may be related to the fluctuations of the magnetic field in the PWN (e.g., [5], [6]).

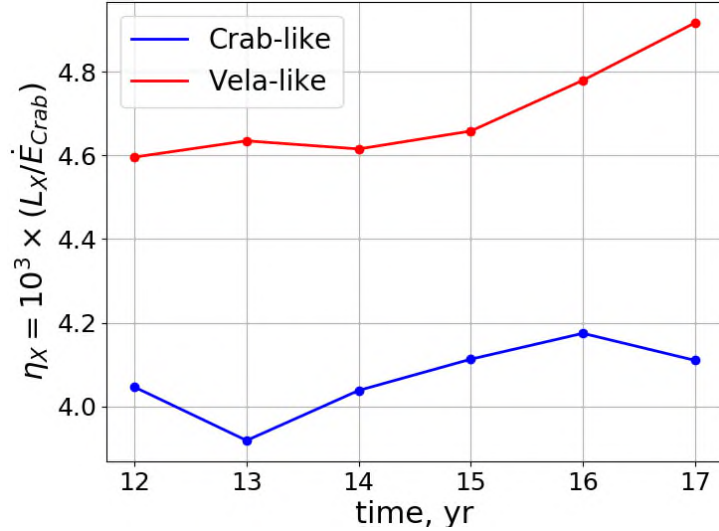


Figure 2: The evolution of integral fluxes of the Crab-like (blue curve) and Vela-like (red curve) model PWNe from Figure 1 between  $t = 12$  and  $t = 17$  yr. The fluxes are expressed through X-ray efficiencies (see, e.g., [1]), assuming the distance and the spin-down luminosity of the Crab pulsar ( $d \simeq 2$  kpc and  $\dot{E} = 5 \cdot 10^{38}$  erg s $^{-1}$ ).

## 2.3. Double-torus PWN: stationary versus transonic models

Accounting for the relative motion of the X-ray PWN and the surrounding matter also facilitates the interpretation of the PWN morphology. Let us take the model of the double-torus Vela PWN, which is believed to interact with a transonic stream of  $M \sim 1.3$  induced by the reverse shock of the supernova [7]. This model ( $\alpha = 80^\circ, \sigma_0 = 0.03$ ) is inflated either (1) into an stationary medium (“stationary model”), or (2) into an oncoming transonic stream of  $M = 1.3$  (“transonic model”). In the latter case, the stream is co-aligned with the PWN axis; see [8] for detail. In Figure 3, synthetic X-ray maps for the cases (1) and (2) are compared to the Chandra X-ray map of the Vela PWN.

It is apparent that the transonic model provides a better match with the morphology of a real nebula. *First*, the arcs (Doppler-brightened parts of the tori) are of similar brightness, while in the stationary model the SE torus is much brighter overall. *Second*, the NW (windward) torus appears larger than the SE (leeward) one. In Vela, its NW arc has a larger extent than the SE arc. *Third*, the far side of the SE torus does not appear that bright as in the stationary model. In Vela, none of the tori has a bright far side. *Fourth*, between the bright arcs begins to show the windward jet of the nebula (see [9] for detail).

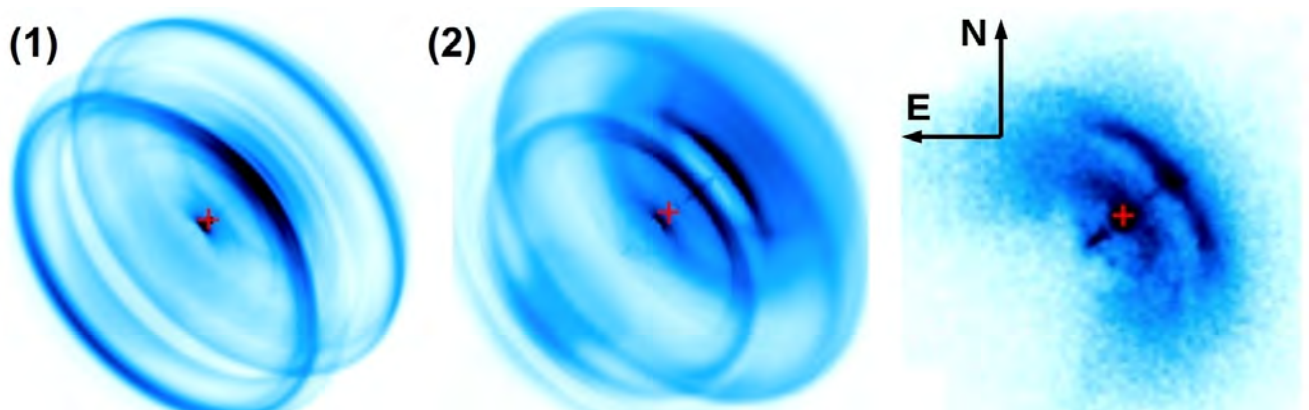


Figure 3: *Left to right:* (1),(2) – synthetic maps of synchrotron X-ray radiation of the double-torus PWN model ( $\alpha = 80^\circ, \sigma_0 = 0.03$ ) for a a “stationary” and “transonic” ( $M \sim 1.3$ ) cases; (3) – the Chandra X-ray map of the Vela PWN. The viewing and position angles are  $\theta_{view} = 120^\circ$  and  $\Psi = 310^\circ$  (E of N) as in the maps in Figure 1.

## Acknowledgements

K.L. acknowledges the support from the baseline project 0040-2019-0025 of the Ioffe Institute. PLUTO simulations of PWNe were performed by G.P. & A.P., supported by RSF grant 21-72-20020. Modelling was carried out partly at the Tornado subsystem of the supercomputer center of Peter the Great St.Petersburg Polytechnic University. The authors are grateful to the PLUTO developers.

## References

1. O. Kargaltsev and G. G. Pavlov, in C. Bassa, Z. Wang, A. Cumming, and V. M. Kaspi, eds., *40 Years of Pulsars: Millisecond Pulsars, Magnetars and More*, *American Institute of Physics Conference Series*, volume 983, 171–185 (2008).
2. A. Mignone, G. Bodo, S. Massaglia, T. Matsakos, O. Tesileanu, C. Zanni, and A. Ferrari, *ApJS*, **170**, 228, 2007.
3. K. P. Levenfish, G. A. Ponomaryov, A. E. Petrov, A. M. Bykov, and A. M. Krassilchtchikov (2021).
4. A. M. Krassilchtchikov, A. M. Bykov, G. M. Castelletti, G. M. Dubner, O. Y. Kargaltsev, and G. G. Pavlov, in *Journal of Physics Conference Series*, *Journal of Physics Conference Series*, volume 798, 012003 (2017).
5. C. A. Wilson-Hodge, M. L. Cherry, G. L. Case, W. H. Baumgartner, et al., *ApJL*, **727**, L40, 2011.
6. M. S. Pshirkov, B. A. Nizamov, A. M. Bykov, and Y. A. Uvarov, *MNRAS*, **496**, 5227, 2020.
7. R. A. Chevalier and S. P. Reynolds, *ApJL*, **740**, L26, 2011.
8. G. A. Ponomaryov, K. P. Levenfish, A. E. Petrov, and Y. A. Kropotina, in *Journal of Physics Conference Series*, *Journal of Physics Conference Series*, volume 1697, 012022 (2020).
9. G. A. Ponomaryov, K. P. Levenfish, A. E. Petrov, and Y. A. Kropotina (2021).